AFRL-RX-WP-TP-2008-4331

COMPRESSION PROPERTY DETERMINATION OF A GAMMA TITANIUM ALUMINIDE ALLOY USING MICROSPECIMENS (Preprint)

W.J. Porter, M.D. Uchic, R. John, and N.B. Barnas

Metals Branch
Metals, Ceramics, and NDE Division

SEPTEMBER 2008
Interim Report

Approved for public release; distribution unlimited.

See additional restrictions described on inside pages

STINFO COPY

AIR FORCE RESEARCH LABORATORY
MATERIALS AND MANUFACTURING DIRECTORATE
WRIGHT-PATTERSON AIR FORCE BASE, OH 45433-7750
AIR FORCE MATERIEL COMMAND
UNITED STATES AIR FORCE

REPORT DOCUMENTATION PAGE

Form Approved
OMB No. 0704-0188

1. REPORT DATE ***(DD-MM-YY)***
September 2008

2. REPORT TYPE
Journal Article Preprint

3. DATES COVERED ***(From - To)***

4. TITLE AND SUBTITLE
COMPRESSION PROPERTY DETERMINATION OF A GAMMA TITANIUM ALUMINIDE ALLOY USING MICROSPECIMENS (Preprint)

5a. CONTRACT NUMBER
IN HOUSE

5b. GRANT NUMBER

5c. PROGRAM ELEMENT NUMBER
62102F

6. AUTHOR(S)
W.J. Porter, M.D. Uchic, R. John, and N.B. Barnas

5d. PROJECT NUMBER
4347

5e. TASK NUMBER
RG

5f. WORK UNIT NUMBER
M02R3000

7. PERFORMING ORGANIZATION NAME(S) AND ADDRESS(ES)
Metals Branch
Metals Ceramics, and NDE Division
Materials and Manufacturing Directorate
Wright-Patterson Air Force Base, OH 45433-7750

University of Dayton Research Institute

8. PERFORMING ORGANIZATION REPORT NUMBER
AFRL-RX-WP-TP-2008-4331

9. SPONSORING/MONITORING AGENCY NAME(S) AND ADDRESS(ES)
Air Force Research Laboratory
Materials and Manufacturing Directorate
Wright-Patterson Air Force Base, OH 45433-7750
Air Force Materiel Command
United States Air Force

10. SPONSORING/MONITORING AGENCY ACRONYM(S)
AFRL/RXLMN

11. SPONSORING/MONITORING AGENCY REPORT NUMBER(S)
AFRL-RX-WP-TP-2008-4331

12. DISTRIBUTION/AVAILABILITY STATEMENT
Approved for public release; distribution unlimited.

13. SUPPLEMENTARY NOTES
PAO case number WPAFB 08-5314, cleared 04 September 2008. The U.S. Government is joint author of this work and has the right to use, modify, reproduce, release, perform, display, or disclose the work. Submitted to Scripta Materialia, September 2008. Paper contains color.

14. ABSTRACT
The room temperature yield behaviors under compression of micro-specimens representing three lamellar orientations of a gamma titanium aluminide alloy were evaluated. The mechanical responses from specimens of each orientation and various diameters are compared to one another and to compression-loaded, conventionally-sized titanium aluminide specimens. The yield stress results from the micro-specimens are shown to be relatively independent of specimen diameter and similar to those of conventionally-sized compression specimens.

15. SUBJECT TERMS
Micro-compression, Titanium Aluminides, yield stress, micro-specimen

16. SECURITY CLASSIFICATION OF: a. REPORT	b. ABSTRACT	c. THIS PAGE	17. LIMITATION OF ABSTRACT:	18. NUMBER OF PAGES	19a. NAME OF RESPONSIBLE PERSON (Monitor)
Unclassified	Unclassified	Unclassified	SAR	16	James M. Larsen **19b. TELEPHONE NUMBER** *(Include Area Code)* (937) 255-9791

Compression Property Determination of a Gamma Titanium Aluminide Alloy Using Micro-specimens

W.J. Porter*, M.D. Uchic, R. John, and N.B. Barnas
Air Force Research Laboratory, Materials and Manufacturing Directorate (AFRL/RXLM),
Wright-Patterson Air Force Base, OH 45433-7817
*University of Dayton Research Institute (UDRI), OH 45469-0020

The room temperature yield behaviors under compression of micro-specimens representing three lamellar orientations of a gamma titanium aluminide alloy were evaluated. The mechanical responses from specimens of each orientation and various diameters are compared to one another and to compression-loaded, conventionally-sized titanium aluminide specimens. The yield stress results from the micro-specimens are shown to be relatively independent of specimen diameter and similar to those of conventionally-sized compression specimens.

Keywords: Micro-compression; Titanium Aluminides; yield stress; micro-specimen

Gamma titanium aluminide (γ-TiAl) alloys have received significant attention as potential replacements for nickel-based superalloys in many aerospace applications. Gamma alloys are noted for their excellent high temperature mechanical properties and oxidation resistance and their mechanical properties compare favorably with many nickel-base alloys on a density-normalized basis [1,2]. A fully-lamellar microstructure, which consists of thin, parallel layers of γ (TiAl) and α_2 (Ti_3Al) phases is an often-desired condition due to its balance of tensile, fatigue and creep properties [3]. Previously, studies of the anisotropic nature of plastic flow in the two-phase lamellar structure have been have been facilitated through the use of polysynthetically-twinned (PST) crystals [4-7] which are akin to single grains of the fully-lamellar γ-α_2 structure and through the use of specimens with large colony structures developed via heat treatment [8,9]. The PST crystals are normally grown using float-zone melting techniques and are generally 'simple' alloys normally having binary (Ti-Al) and, on occasion, ternary (Ti-Al-X) compositions. However, the chemistries of the PST alloys are generally not representative of the multi-element alloys being considered for use in engineering (applications).

The recent development of fabrication and testing techniques suited for micron-size specimens potentially allow for the investigation of mechanical properties of engineering alloys on a grain and sub-grain level [10-12]. This study was performed to determine whether the use of micro-specimen testing could obviate the need to develop boutique alloys for macro-scale experimental purposes, such as the aforementioned γ-TiAl PST. Specifically, micro-compression specimens were prepared from within three colonies of differing lamellar orientation of a bulk polycrystalline sample with a complex (5-element) composition. The diameters of the micro-specimens were varied to determine whether size effects are a factor in material response. The mechanical response of the different orientations is finally compared to PST materials.

The alloy used in this study had a nominal chemistry of Ti-46.5Al-3Nb-2Cr-0.2W [13]. To achieve the large colony, fully lamellar microstructure shown in Fig. 1, the material was heat treated in air at 900°C for 24 hours and then air cooled. Details on material preparation can be found in [8].

Orientation imaging microscopy (OIM) was used to identify the crystallographic nature of the three adjacent colonies interrogated in this study. The orientations, defined as the angle of the lamellae with respect to the compression axis (0°= parallel, 90°= normal), for each colony were 48, 65 and 69º.

After identifying the colonies of interest, the micro-specimens were machined using a sequence of micro-electro-discharge machining (micro-EDM) and focused-ion-beam (FIB) milling [10]. The use of micro-EDM machining enabled the preparation of micro-compression samples that are much larger than has been typically been reported in the literature, ranging from 35-80 microns in diameter and 80-160 microns in length. This size-scale was desired in order that the micro-samples contained many lamellae, and also to potentially minimize other possible size-scale effects. The recast layer produced by the micro-EDM process was removed by FIB milling [12]. Figure 2a and 2b show a representative sample after the micro-EDM and FIB milling steps, respectively. The aspect ratio (L/D) for all of the specimens ranged from 1.7:1 to 2.4:1, and the dimensions for all of the specimens prior to testing are shown in Table 1.

The specimens were tested using an MTS NanoXP Nanoindenter outfitted with a conical diamond flat-punch indention tip [12]. All of the tests in this study were performed at room temperature using a displacement rate of 8nm/s. Axial deformation was limited to just below 5% strain to minimize gross deformation of the specimens.

The stress-strain curves for all of the specimens tested in this study are shown in Figure 3 and are grouped according to lamellar orientation. For the 48° orientation, three of the four specimens exhibited comparable elastic responses up to approximately 150 MPa and plastic responses up to 240 MPa. The flow curves for the specimens loaded to 4 and 4.75% strain (K5024 and K5025, respectively) had very similar shapes, mimicking one another to their maximum loading points and a near identical response upon unloading. The unloading curve of specimen K5010 also had a similar slope to these specimens. The load and unload response of the fourth specimen, K5006, was significantly different from the other three. The loading portion of K5006 could be indicative of a cracked specimen although no outward signs of cracking were apparent. No conclusive reason(s) for the behavior of this specimen has been identified.

All of the specimens with the 65° orientation exhibited a linear response upon loading just beyond 220 MPa. Also noteworthy of the 65° specimens is the similarity in flow behavior despite the almost 1.8 times difference in diameter from the smallest specimen to the largest. The 65° specimens were greater than the 48° and slightly higher than the 69° specimens in terms of strength.

The overall compressive behavior of the 69° specimens exhibited the least scatter of the three orientations. As shown in Fig. 3c, the linear portions of all seven stress-strain curves agree well up to 180MPa and the plastic region is in decent agreement up to 230MPa. The 69° specimens represent diameters ranging from almost 42 to 80 microns in diameter, similar to the 1.8 times difference in the 65° specimens. The three largest diameter specimens displayed very similar yield behavior to beyond 4% strain. Importantly, specimen K5013, a 43.1 micron diameter specimen tested to just below 2% strain, revealed very similar flow behavior when compared to the larger diameter specimens, precluding any obvious size dependence effects for this set of data. The 69° specimens demonstrated consistently higher strengths than the 48° specimens and similar strengths to the 65° specimens.

A feature common to all of the flow curves is the presence of strain bursts (i.e. an abrupt increase in strain at a given stress level) along the loading portion of the stress-strain curve. As shown by all of the stress-strain curves in Figure 3, the strain bursts usually occur towards the upper end of the elastic region and throughout the plastic region of the stress-strain curve. Strain bursts have been associated with sudden gross slip activity throughout a specimen upon loading [10-12]. Deformed specimens from each orientation are shown in Figure 4. The slip planes activated during compression are apparent on the surface of each specimen. The majority of the slip planes shown in Figure 4 are localized to the gage section of the specimen with a couple of slip planes intersecting the top surface (in contact with micro-indenter) of the 48° and the 69° specimens. At the size scales investigated in this study, the diameter of the specimen does not seem to play a role in determining where slip will occur. The specimens in Figure 4 a-c have

diameters ranging from 41.2 to 43.1 microns and the diameter of the specimen in Figure 4d is 75.7 microns, yet the nature of the slip activity in each is indistinguishable.

To illuminate where slip is occurring within our specimens, the FIB was used to longitudinally slice a compressed specimen, K5012, in half. A comparison of Fig. 5a) secondary and Fig. 5b) backscattered images are shown. The flat surface provides for higher quality images than possible when imaging a cylindrical surface. The surface displacements associated with slip are highlighted in Figure 5a by the arrows. In this case, two prominent slip planes were active with the upper slip plane intersecting the surface that was in contact with the indenter tip (indicating that the surface was not in perfect contact with the flat-punch tip at the start of the test). The lamellar phases are highlighted by the backscattered conditions used in Figure 5b. The darker contrast (lower density) material is the γ phase (TiAl) and the lighter contrast (higher density) material is the α_2 phase (Ti_3Al). From Figure 5, slip is shown to take place near a $\gamma/\ \alpha_2$ interface in both cases. For the orientations investigated in this study, deformation is isolated only to the γ phase lamellae [4,6,14,15]. As loading is increased, dislocation pile-up in the γ phase leads to stress incompatibility at the boundaries along the $\gamma/\ \alpha_2$ interface, leading to slip parallel to the lamellar orientation. The slip planes shown in Figure 4 and 5 are believed to have formed in this manner.

As mentioned, PST crystals exhibit significant yield anisotropy as a function of lamellar orientation to loading direction. The anisotropy is evident under tensile and compressive loading conditions [5]. The anisotropic behavior of lamellar γ -TiAl is highlighted by the data shown in Figure 6. This figure clearly shows the sensitivity of the yield behavior of the inclination of the lamellar structure relative to the loading direction. The average yield stress, indicated by the closed circles, and associated data spread for each orientation in this study is shown in Figure 6. The average yield stress show a marked increase (~90MPa) from the 48 orientation to the 65 orientation and a modest decrease (~35MPa) from 65° to 69°. While the decrease in average yield stress from 65 to 69 is counter to published findings, it is important to note that the difference in orientation between these specimens is subtle and that the maximum yield stress measured in each population is the same. Also, the higher overall yield stress averages for both the 65 and 69 specimens, when compared to the 48 specimens, is consistent with the literature [4, 13].

Size scale effects on yield behavior within the micro-specimens in this study were found to be minimal. The curves from the literature shown in Figure 6 were constructed from experiments using conventionally-sized specimens. The data from [6] was generated using specimens with a 3mm x 3mm cross section by 6mm long. The data from [14] was collected using specimens with a 5mm x 5mm cross section and 10mm long. As stated earlier, a major issue with the γ-TiAl family of alloys is their general lack of room temperature ductility, especially in polycrystalline form. A significant amount of research has been undertaken to address the ductility shortcoming with little effect on baseline (i.e. binary/ternary) alloy strengthening. Such is the case with the Ti-46.5Al-3Nb-2Cr-0.2W alloy (this study) where the Cr and Nb additions are meant primarily for plasticity enhancement [1,15]. Therefore, it is interesting to note that the yield properties of the micro-specimens are very similar to those of the binary alloys, Ti-49.3Al and Ti-48.1Al, shown in Figure 6. Comparing the yield properties for the conventionally-sized specimens [6,14] and for the micro-specimens from this study reveals no clear size scale dependency.

Micro-compression specimens from a complex, gamma titanium aluminide polycrystalline alloy were fabricated and tested at room temperature. The specimens represented three grains with lamellar orientations ranging from 48° to 69°. Specimen diameters were varied from approximately 40 microns to 80 microns to investigate size scale effects. Compression testing resulted in consistent yield properties that compared favorably to conventionally-sized specimens in terms of both strength (i.e. no size scale dependency) and the effect of lamellar orientation.

This work was performed at the Air Force Research Laboratory (AFRL/RXLM), Materials and Manufacturing Directorate, Wright-Patterson Air Force Base, OH 45433-7817 under on-site contract number FA8650-04-C-5200. The authors gratefully acknowledge the support of Dr. Victor Giurgiutiu of the Air Force Office of Scientific Research (AFOSR) under task 2306-6M2AL8. We appreciate the generosity of Dr. Y-W Kim (UES, Inc.) for supplying the material.

References

[1] Y-W. Kim, J. Metals 41 (1989) 24.
[2] Y-W. Kim and Dimiduk, D.M., J. Metals 43 (1991) 40.
[3] Y-W. Kim, Acta Metall. Mater 40 (1992) 1121
[4] M. Yamaguchi and Y. Umakoshi, Prog. Mater. Sci. 34 (1990) 1.
[5] H. Inui, M. H. Oh, A. Nakamura and M. Yamaguchi, Acta Metall. Mater. 40 (1992) 3095.
[6] T. Fujiwara, A. Nakamura, M Hosomi, S.R. Nishitani, Y. Shirai and M. Yamaguchi, Philosophical Magazine A, 61, 4 (1990) 591.
[7] D. J. Larson, M. K. Miller, H. Inui and M. Yamaguchi, ORNL/ CP-96517.
[8] R. John, W.J. Porter, III, and S. Olson, Intermetallics 12 (2004) 1.
[9] W.J. Porter, III, R. John, and S. Olson, Scripta Materialia 49 (2003) 327-332.
[10] M.D. Uchic, D.M. Dimiduk, J.N. Florando and W.D. Nix, Science 305 (2004) 986.
[11] M.D. Uchic and D.M. Dimiduk , Mat. Sci. & Engrg A 400-401 (2005) 268.
[12] M.D. Uchic, D.M. Dimiduk, R. Wheeler,P.A. Shade, H.L. Fraser, Scripta Materialia 54 (2006) 759.
[13] Y-W. Kim, J. Metals 46 (1994) 30.
[14] T. A. Parthasarathy, M. G. Mendirratta, and D. M. Dimiduk, Acta Mater. 46, 11 (1998) 4005.
[15] M. Yamaguchi H. Inui, in: Darolia et al (Eds), Structural Intermetallics, TMS, Warrendale, PA, 1993, pp. 127-142.

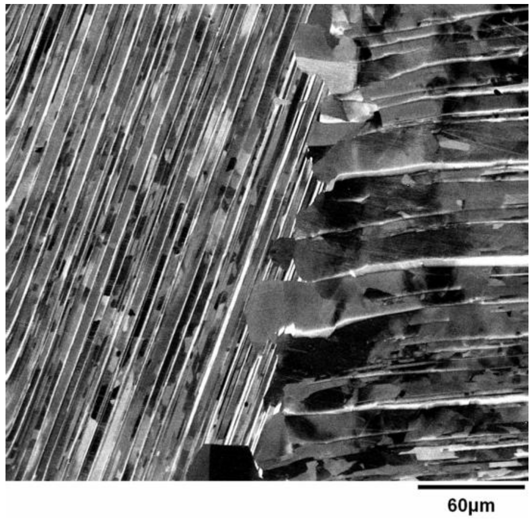

Figure 1. Representative micrograph of fully lamellar microstructure after 900°C/ 24hr/air cool. Dark contrast phase is γ; light contrast phase is α_2.

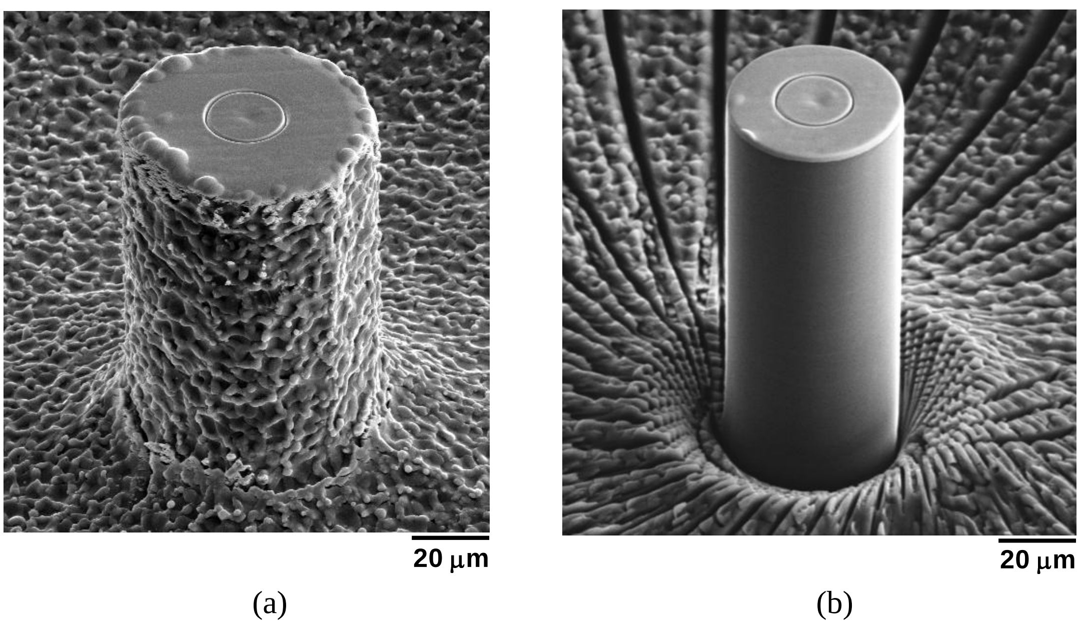

Figure 2. Specimen shown before (a) and after (b) recast layer removal via focused ion beam (FIB) milling.

Table 1: Micro-specimen orientation and dimensional information.

Specimen ID	Orientation (°)*	Diameter, D (μm)	Height, L (μm)	Aspect Ratio, L/D	0.2% Yield Stress, (MPa)
K5023	48	35.3	76.6	2.2	240
K5006	48	41.3	87.8	2.1	175
K5010	48	41.3	98.7	2.4	180
K5024	48	41.8	73.7	1.8	180
K5008	65	41.2	98.7	2.4	280
K5009	65	43.5	94.1	2.2	280
K5005	65	50.1	107.8	2.2	300
K5025	65	75.7	133.4	1.8	260
K5011	69	42.6	91.4	2.1	260
K5012	69	43.0	80.4	1.9	220
K5013	69	43.1	81.8	1.9	265
K5003	69	46.4	109.6	2.4	225
K5021	69	67.7	141.0	2.1	300
K5020	69	68.8	136.9	2.0	220
K5022	69	79.7	134.1	1.7	280

*angle of lamellae wrt compression axis; 0°= parallel, 90°= normal

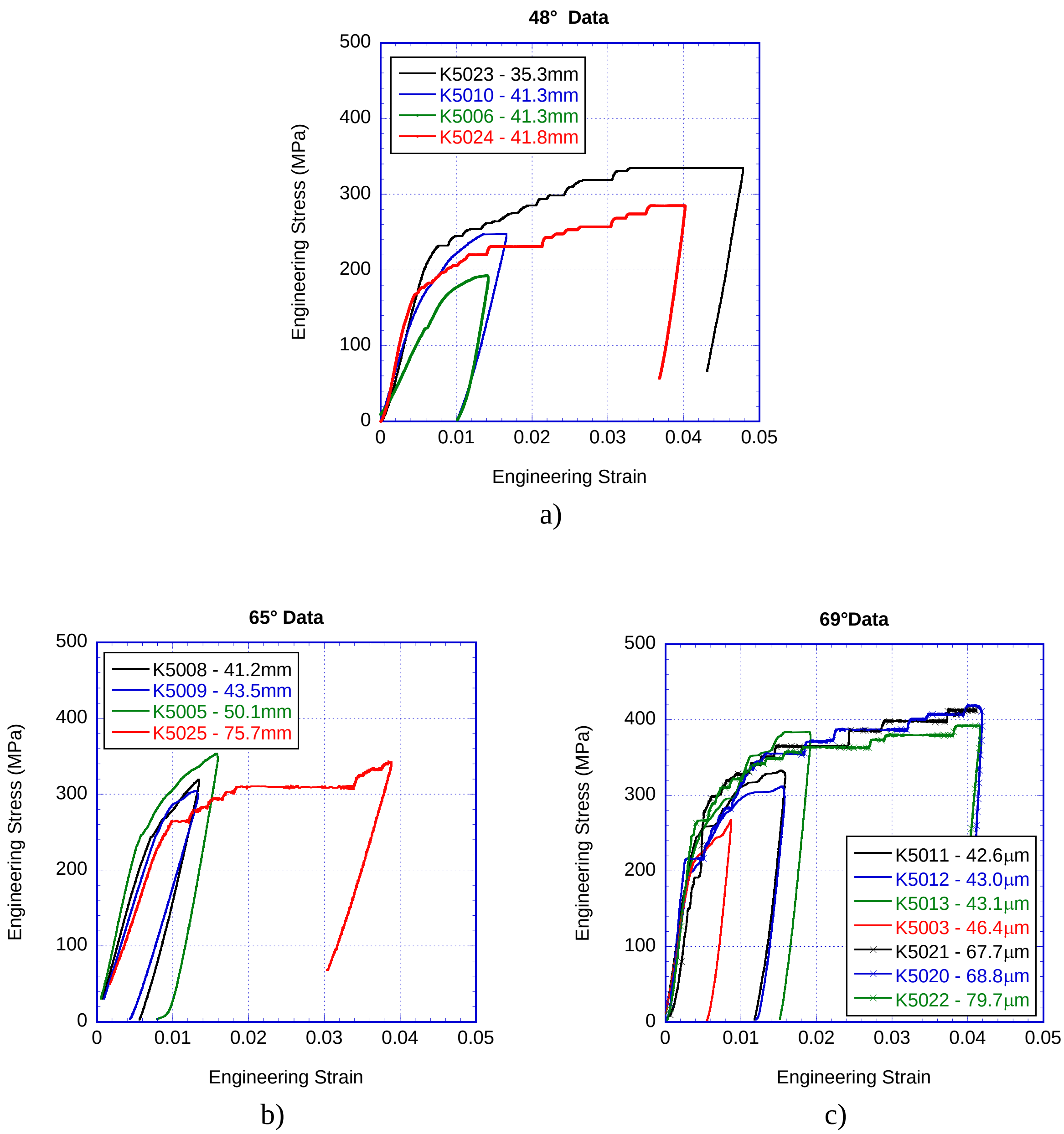

Figure 3. Stress-strain response for micro-specimens with orientations of a) 48°, b) 65°, and c) 69°.

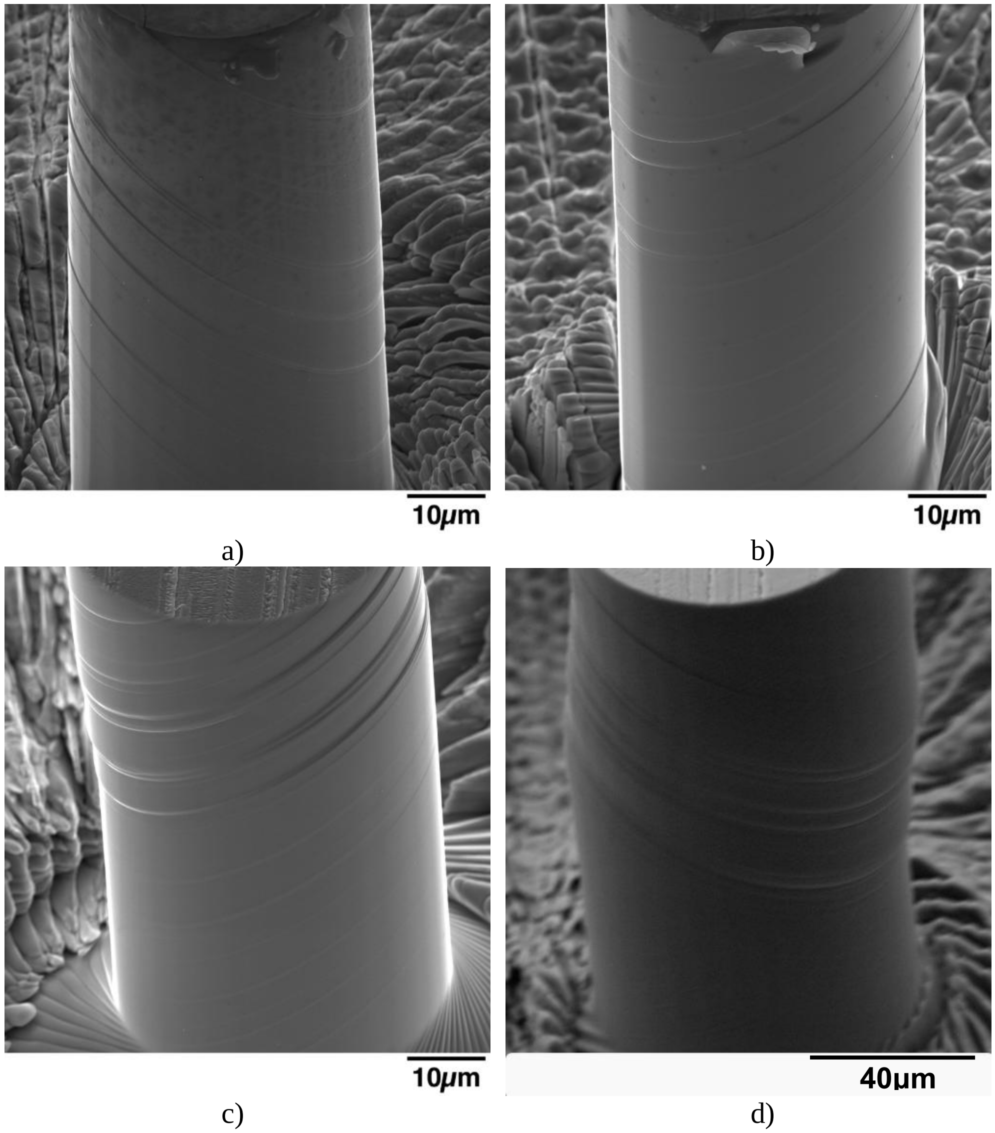

Figure 4. Specimens after compression testing: a) K5006-48º-41.3μm, ~1.5% plastic strain, b) K5008-65º-41.2μm, ~1.5% plastic strain) K5013-69º-43.1μm, ~2% plastic strain, and d) K5025-65 º -75.7μm, ~4% plastic strain.

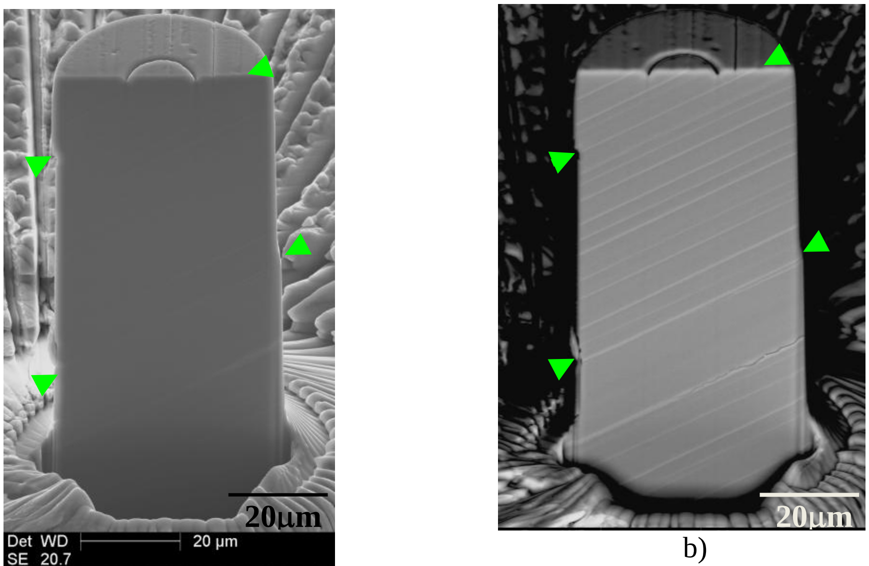

b)

Figure 5. a) Secondary and b) backscattered electron images of Specimen K5012 (69º-43.0µm, plastic strain ~1.5%). Specimen has been halved to reveal displacement from slip and coincidence of slip with α_2 (light contrast) and γ (dark contrast) lamellar interfaces. Deformation primarily occurs in the gamma phase at the boundary region between the α_2 and γ lamellar interfaces.

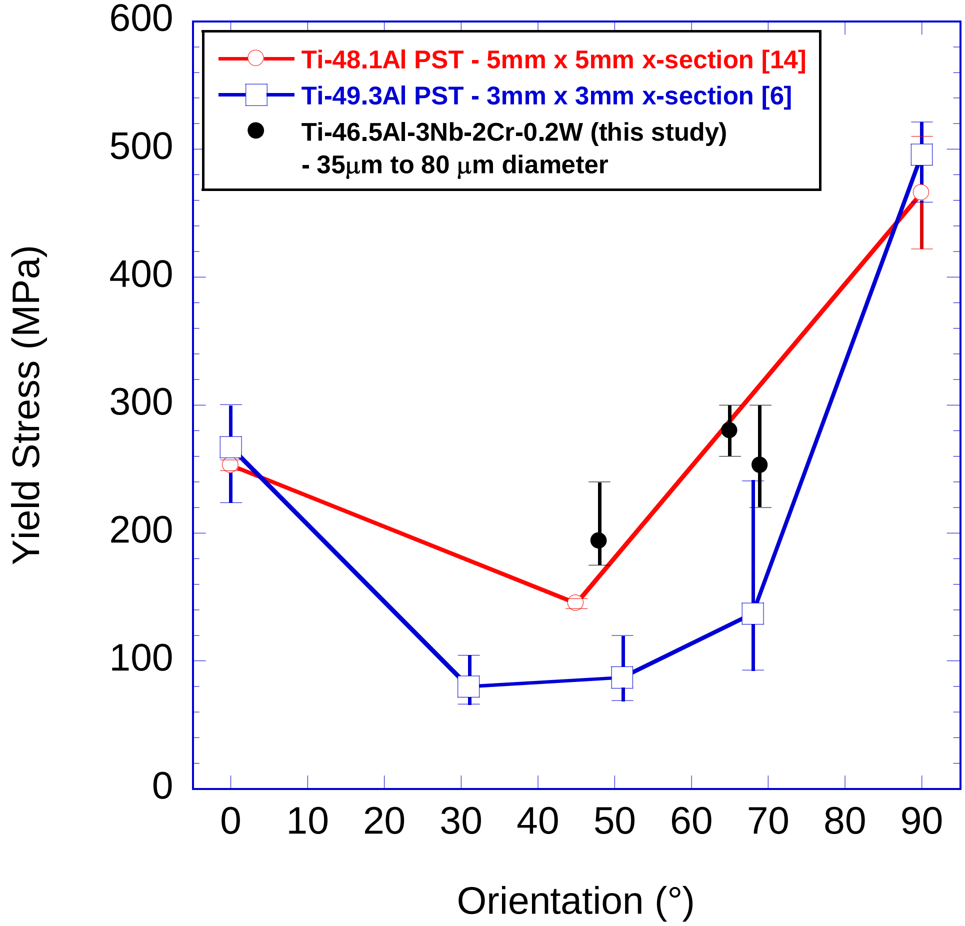

Figure 6. Comparison of compression yield data from this study to published PST data. Note that the trend in the yield data from the micro-specimen tests is similar to that found in conventionally-sized specimens.